

See discussions, stats, and author profiles for this publication at: <https://www.researchgate.net/publication/333559132>

Small scale flying demonstration of semi aeroelastic hinged wing tips

Conference Paper · June 2019

CITATIONS

0

READS

215

4 authors, including:



[Thomas Wilson](#)

Airbus

28 PUBLICATIONS 93 CITATIONS

[SEE PROFILE](#)



[Andrea Castrichini](#)

Airbus

22 PUBLICATIONS 85 CITATIONS

[SEE PROFILE](#)

Some of the authors of this publication are also working on these related projects:



Airbus/Ariane Sloshing Symposium [View project](#)



ALPES Project - Aircraft Loads Prediction using Enhanced Simulation [View project](#)

SMALL SCALE FLYING DEMONSTRATION OF SEMI AEROELASTIC HINGED WING TIPS

Thomas Wilson, James Kirk, John Hobday & Andrea Castrichini

*Airbus Operations Ltd, United Kingdom
thomas.wilson@airbus.com
james-graham.kirk@airbus.com
john.hobday@airbus.com
andrea.a.castrichini@airbus.com*

Keywords: Aeroelastic, flutter, load alleviation, gusts, manoeuvres, hinged / folding wing tips, semi aeroelastic hinge, flying demonstrator, flight testing, AlbatrossONE

Abstract: The primary purpose of a hinged wing tip on an airliner aircraft is to allow an aerodynamically efficient high aspect ratio wing to enter an airport gate of standard dimensions. There exists a potential opportunity to allow a wing tip to move in flight to alleviate the loads and achieve a lower wing weight – or enable the wing span to be maximised. This technology has become known as the “Semi Aeroelastic Hinge”. This paper will present the AlbatrossONE Semi Aeroelastic Hinge small scale demonstrator aircraft and the results from the wind tunnel tests and the first flight tests.

1. INTRODUCTION

Folding wings have long been a reality in naval aviation to allow fixed wing aircraft to be stored in confined spaces on aircraft carriers. The concept of applying the same technology to large civil aircraft is not new, and now the industry is developing a long range aircraft that will include a wing span extension of the order of 7m with the objective of achieving a performance improvement via a reduction in induced drag, but will be able to access the standard 65m gate thanks to a folding mechanism. However, wing weight increases for such an aircraft can be expected due to the longer wing, the folding mechanism, and above all the reinforcement of the existing wing to resist the higher bending loads from the greater span.

It has been recognised that the hinge associated with folding a wing tip on the ground could in principle also be used in flight for the purpose of load alleviation, thus enabling a wing span increase and drag improvement with a much lower increase in loads and weight. Moreover although many possibilities exist for realising a hinged, load alleviating wing tip, the path favoured by researchers at Airbus is to exploit the key property of an ideal hinge, which is simply that it does not transmit bending moment [1 & 2]. By combining the free hinge with a lock and a clutched actuator, an active / passive / adaptive system is envisaged whereby the wing tip can be released in response to a severe gust or manoeuvre, but then “recovered” to its planar position afterwards to continue efficient flight. This technology has become known as the “**Semi Aeroelastic Hinge**”.

Much theoretical work has been done to understand the basic physics of a freely folding wing tip [1 & 3-7], including how the orientation of hinge axis – the “flare angle”, see figure 1 – can be used to avoid flutter [1 & 4] and the levels of load alleviation that appear to be achievable, approaching 20% in terms of wing root bending moment [1 & 4]. In addition the inherent static

and dynamic stability of a freely folding wing tip (with a flared hinge), when behaving as a single degree of freedom, has been verified by wind tunnel tests at the University of Bristol [8].

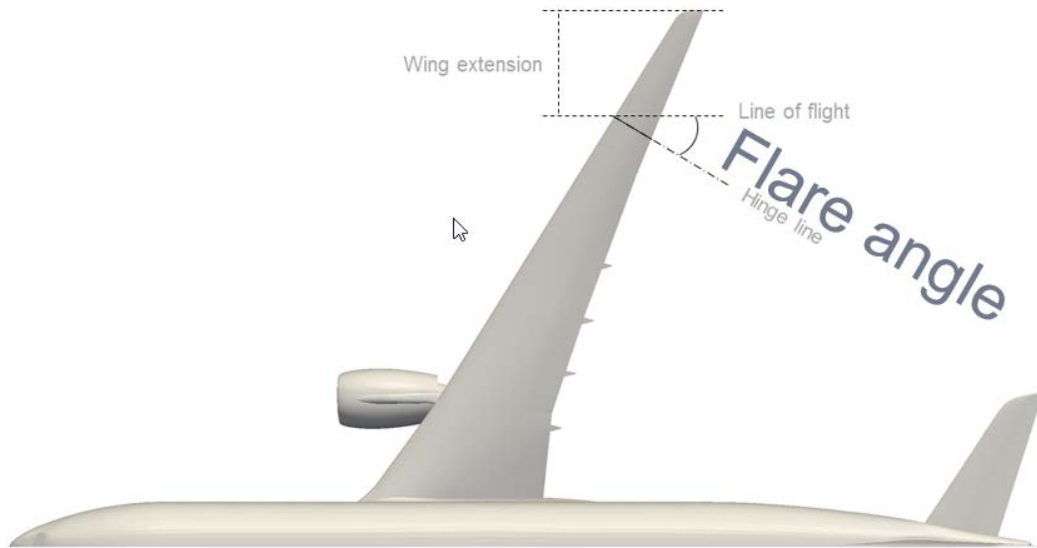


Figure 1: Definition of the hinge flare angle

The next step was to demonstrate the Semi Aeroelastic Hinge with a **small scale flying demonstrator**, known as “AlbatrossONE” which is shown in figure 2. This paper will present the details of the aircraft and the results from the wind tunnel tests and the first flight tests.



Figure 2: AlbatrossONE, Semi Aeroelastic Hinge Demonstrator

2. EXPECTED FINDINGS FROM THE FLYING DEMONSTRATOR

AlbatrossONE is intended to be a basic proof of concept demonstrator for the Semi Aeroelastic Hinge technology. So although the aircraft is geometrically scaled to represent a possible future full scale aircraft, it is **not** dynamically scaled for either handling qualities and/or aeroelasticity in terms of mass and stiffness properties, nor of course will it fly in the Mach range that airliner aircraft are designed for. Therefore the aircraft is intended to provide a *qualitative* rather than a quantitative demonstration of the various aspects of physical behaviour associated with the semi aeroelastic hinge concept, including:

- ⇒ Near-linear variation of the symmetric and anti-symmetric wing tip flapping mode frequencies with airspeed. Figure 3 gives an example of this predicted behaviour for a full scale A321-like aircraft with wing tip extensions [4].

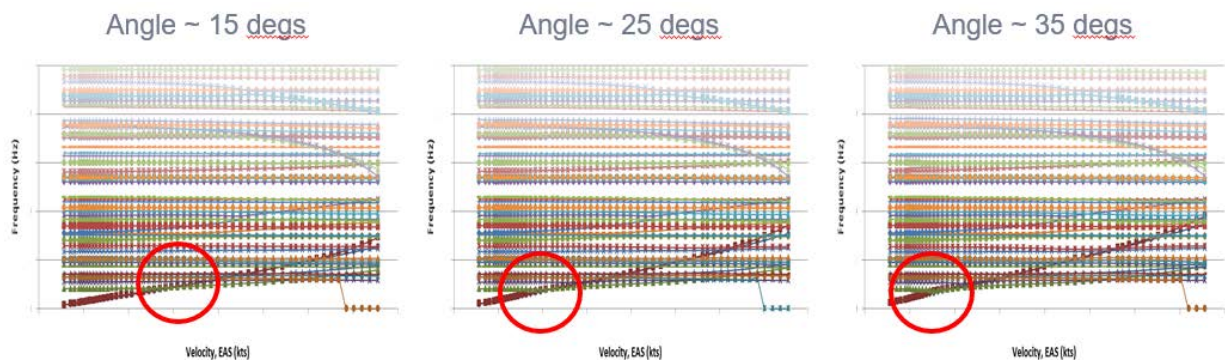


Figure 3: Frequency versus airspeed for hinge flare angles of 15°, 25° and 35°

- ⇒ Static and dynamic stability of the free wing tip [8].
- ⇒ The increase of the free wing tip fold angle – the “coasting angle” – with aircraft angle of attack.
- ⇒ Reduction of the wing loads when the wing tip is free to fold. Figure 4 gives an example of this predicted behaviour for a full scale A321-like aircraft with wing tip extensions [4].
- ⇒ Near immediate reduction in wing loads when the hinge is released, including consequent aircraft pitch-up response [10]. Moreover the elevator compensation will be demonstrated.
- ⇒ Demonstration of using an actuator to recover the wing tip to its planar position.
- ⇒ Avoidance of separated flow at high aircraft incidence when the wing tip is coasting.
- ⇒ No contact between the wing tips and the ground when the aircraft lands with freely hinged wing tips [11].
- ⇒ Reduction in roll damping when the wing tips are free to fold. Figure 5 gives an example of this predicted behaviour for a full scale A321-like aircraft [4].

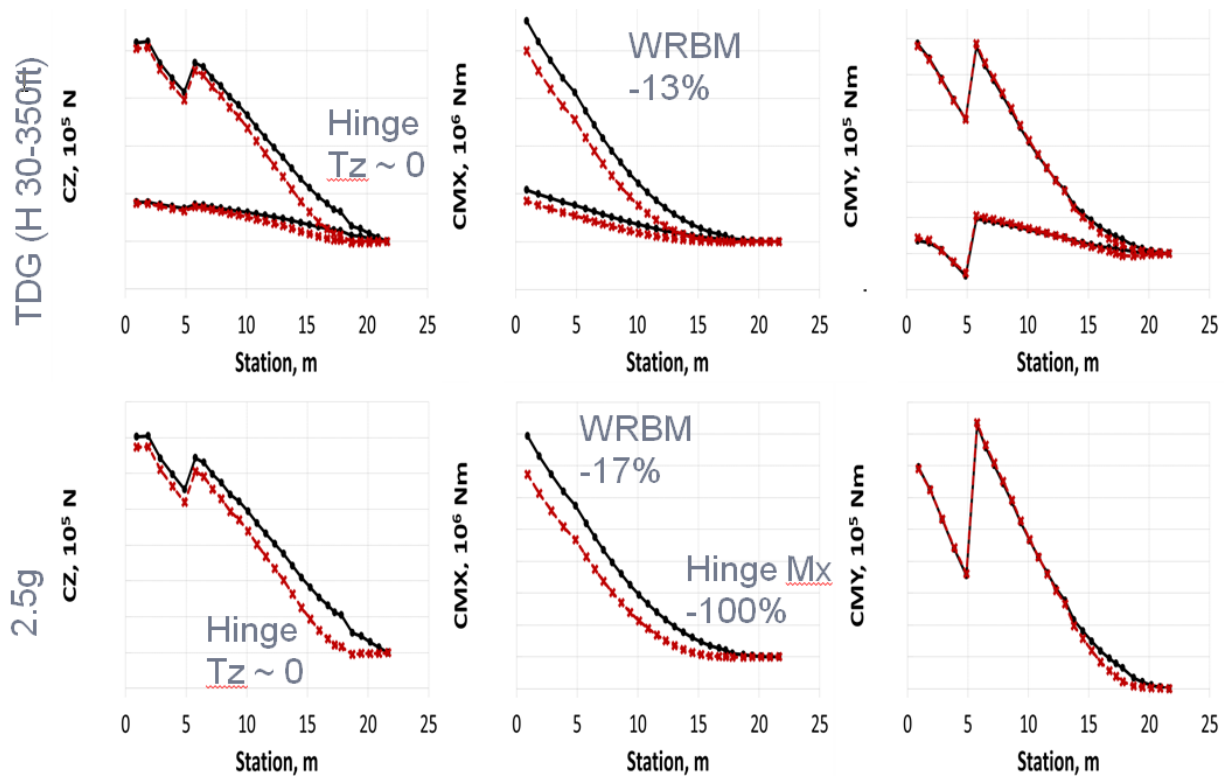


Figure 4: Gust and manoeuvre wing loads for fixed (black) versus free (red) hinged wing tip

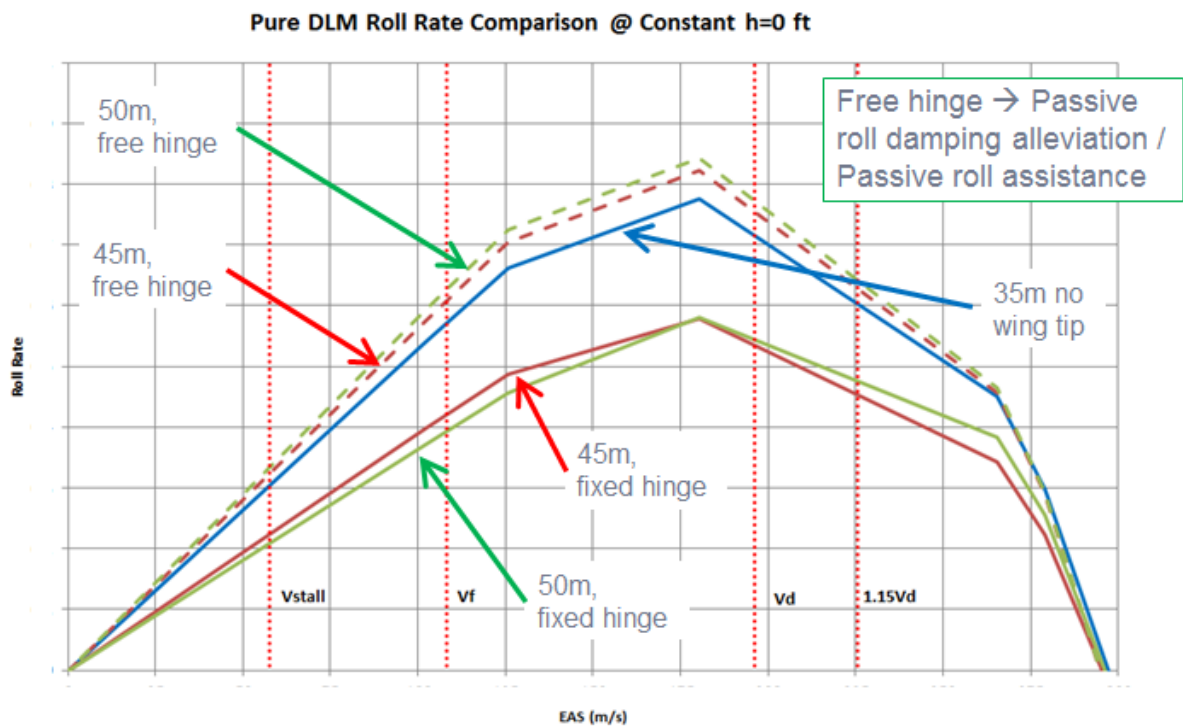


Figure 5: Steady roll rate 'bookcase' simulation for unit aileron deflection for 45m and 50m wings with fixed and free hinged wing tips, plus a 35m wing without wing tip

3. AIRCRAFT OBJECTIVES

Although the Semi Aeroelastic Hinge offers the potential to improve the fuel efficiency of an aircraft there are significant technical challenges posed by allowing a wing tip to flap freely and the necessity to be able to return the wing tip to a planar position after a gust encounter for continued efficient flight. Therefore the overall objective is essentially to show that the Semi Aeroelastic Hinge is a serious proposition based on sound physical principles.

In terms of detailed objectives the AlbatrossONE aircraft is intended to demonstrate that the wing aspect ratio of an Airbus-like aircraft could be *approximately doubled* without the usual detrimental impact on loads and handling qualities thanks to semi aeroelastically hinged wing tips. This demonstration will cover physical effects described in section 2, and also the main functions of the system including the in-flight “release” and “recovery” of the wing tips. These objectives are shown diagrammatically in figure 6.

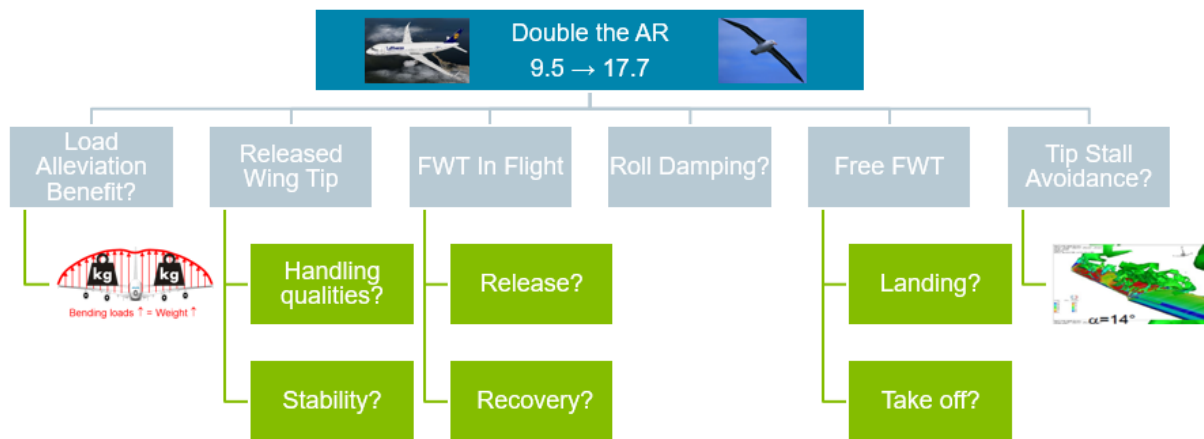


Figure 6: AlbatrossONE objectives

4. DESIGN AND MANUFACTURE

The wing of AlbatrossONE is based on a generic short range aircraft, and is approximately 1:14 scale. The wing has five wing tip configurations:

- ⇒ A 2.6m wing span with no wing tips, equivalent to a 35m wing span.
- ⇒ A 3.2m wing span with fixed (i.e. locked) wing tips, equivalent to a 45m wing span.
- ⇒ A 3.2m wing span with the wing tips free to rotate about their hinges.
- ⇒ A 3.7m wing span with fixed (i.e. locked) wing tips, equivalent to a 52m wing span.
- ⇒ A 3.7m wing span with the wing tips free to rotate about their hinges.

Note that the aspect ratios of the three wing spans are approximately 9, 14 and 18. The wing section is a PSU-90-125WL sailplane aerofoil: 12.5% max thickness at 35.1% chord, 2% max camber at 54.4% chord. The flaps are connected to the wing via dropped hinges. The wing tip hinge flare angle is approximately 15 degrees.

The fuselage is based on the Airbus A321, as are the horizontal tailplane (HTP) and vertical tailplane (VTP) but oversized by 10% in the linear dimensions to increase directional stability.

The wing skins are constructed with Carbon Fibre Reinforced Plastic (CFRP) stiffened with Rohacell foam. The spars are constructed from plywood wrapped in CRFP. The mid and outer wings are detachable from the inner wing with the attachments constructed in titanium with the additive layered manufacturing (ALM) technique. The landing gear attachments and the wing hinges are also constructed in titanium. The landing gears are fabricated from aluminium (with water as the working fluid to provide the required damping), with a pneumatic braking system. The HTP and VTP are made from Rohacell foam wrapped in CFRP. Lastly the fuselage is built from a fibre glass shell supported by plywood frames. The structure is sized to 2.5g / -1g vertical acceleration, with an ultimate factor of 3. Figure 7 shows the wing limit load static test.

The overall weight of the aircraft is approximately 19Kg, which is under the UK Civil Aviation Authority (CAA) limit of 20Kg, above which the aircraft has to be certified. Other relevant CAA regulations include a maximum altitude of 400ft and a maximum line-of-sight distance from the pilot of 500m.

The aircraft is powered by two electric ducted fan motors, which each provide approximately 50N of maximum thrust and a power of 2.7kW. Two 22.5v lipo batteries allow an estimated maximum flight endurance of 10 minutes. The cruise speed of the aircraft is 25m/s and the maximum rated speed is 40m/s.



Figure 7: Wing limit load static test

It is important to reiterate that AlbatrossONE has not been designed so that it necessarily has the physical properties of the full size aircraft, other than the wing tip hinge not passing bending

moment when released. Therefore the aircraft behaviour, and the handling qualities, loads, static aeroelastic and dynamic aeroelastic characteristics related to the free wing tips in particular, can be considered to be only representative of the full size aircraft in a qualitative sense.

Finally note that the name, AlbatrossONE, has been chosen for two reasons. Firstly the wing span and aspect ratio of the largest Albatrosses approach 3.7m and 18, respectively. Secondly the Semi Aeroelastic Hinge concept is superficially analogous to the biomechanics of the Albatross. Albatrosses are able to travel distances of hundreds of kilometres through gliding and “dynamic soaring” flight, and consequently they must maintain spread-wing posture for prolonged periods of time. This is achieved, in part, by a locking mechanism at the shoulder comprised of a sheet of tendons [9]. Simply put, for efficient gliding flight the Albatross locks its shoulder, and when it needs to flap its wings (for propulsion, rapid manoeuvres, responding to turbulence, etc) it unlocks its shoulder.

5. CONTROL SYSTEM

The aircraft is piloted remotely. The pilot and co-pilot control the aircraft via two ground radio transmitters, which are linked to three radio receivers on the aircraft: Transmitter #1 is linked to receivers #1 and #2, and transmitter #2 is linked to receiver #3. With transmitter #1 the pilot commands the primary flight controls: Ailerons, elevators, rudder, “throttle”, main landing gear brakes and nose wheel steering. The controls are partitioned into two independent blocks so that the aircraft can still be controlled should one of the on board receivers fail. With transmitter #2 the co-pilot commands the emergency parachute and the folding wing tip hinge release and recovery mechanism (not yet installed on the aircraft). The parachute can only be safely deployed above 150ft and it is intended to be used in case of a total loss of control of the aircraft, or a failure of transmitter #1 or receivers #1 and #2. If there is a failure of both transmitters or all three receivers then the aircraft automatically enters a shallow spiral dive in order to ensure that it comes down within the operational area. The control system is schematically shown in figure 8.

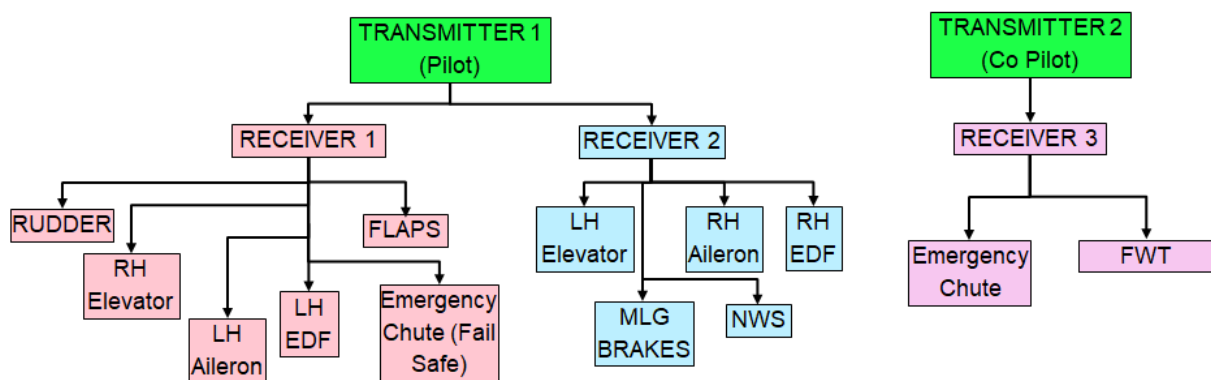


Figure 8: Aircraft control system

6. FLIGHT TEST INSTRUMENTATION

The aircraft is equipped with flight test instrumentation (FTI). For the research aspects of the project the key instruments are the strain gauges and the aircraft accelerometers, which allow the wing loading to be correlated with the aircraft load factor. There are four strain gauges on each wing, located at approximately 10% (wing root), 35%, 55%, and 75% (inboard of hinge) of the semi span (based on the 3.2m / 45m span), which were calibrated prior to each flight by applying

a known load to the wing. The aircraft accelerometer is located close to the centre of gravity. Other important instruments for both the research and aircraft safety include the pitot tube (for airspeed), the alpha and beta vanes on the nose of the aircraft, the barometer (for altitude) and the battery voltage. For the wind tunnel tests (see section 7.) the wing tip was equipped with an accelerometer, however for technical reasons that was not available for the first flight tests. A full list of the FTI can be seen in figure 9.

The data from the FTI was processed and recorded by a set of Arduino computers stacked in the “black box” and by an off-the-shelf Pixhawk computer which can be commonly found in recreational radio controlled aircraft and drones. A telemetry system allowed the data to be viewed live at the ground station during the flights.

In addition to the FTI listed in figure 9 a video camera was mounted at the top of the VTP in order to visually track the movements of the wing tips. A video camera was also used to film the aircraft from the ground. In addition an anemometer was used to assess the latest wind speed and direction at the airfield.

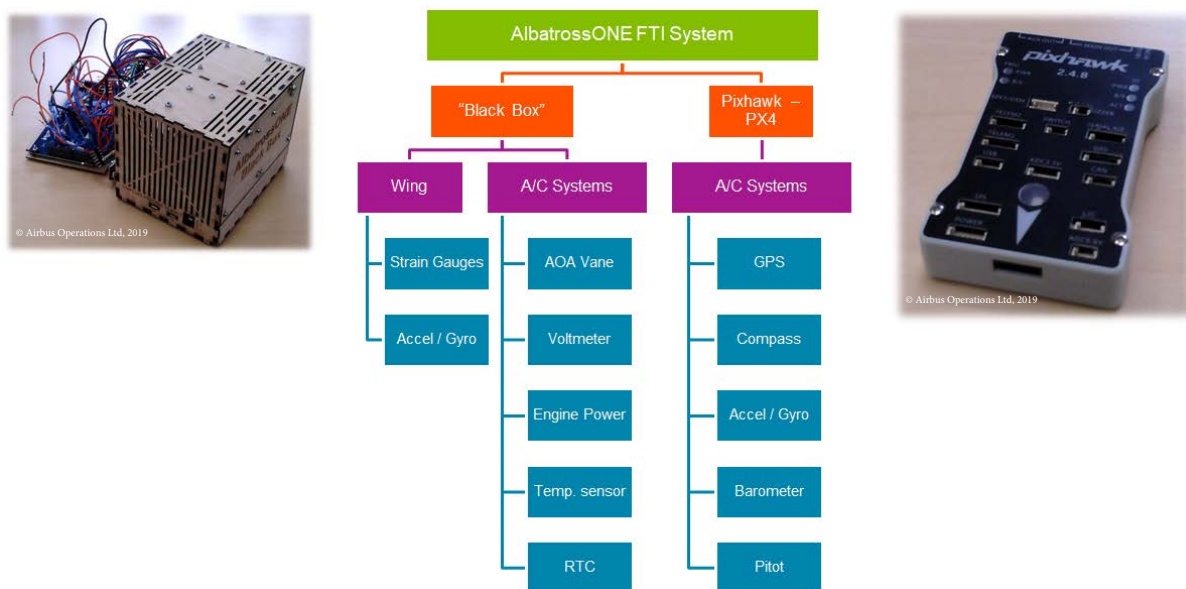


Figure 9: Flight test instrumentation

7. WIND TUNNEL TESTS

Prior to flight testing a wind tunnel test campaign was performed with the following objectives:

1. To check that the flapping frequency of the free wing tips (“45m” and “52m”) are well separated from the first wing bending frequency of the wing for the operational airspeed range. By ensuring this frequency separation the wing tip flapping mode and the wing bending mode are not able to couple and cause flutter. A subsidiary objective is to check that the evolution of wing tip flapping frequency with airspeed is more or less linear as predicted by the models for the full size aircraft [4].
2. To check the range in the “coasting” (or fold) angle of the free wing tips (“45m” and “52m”) for the operational ranges of airspeed and aircraft angle of attack.

Regarding the first objective it is worth noting that for a full size aircraft it is effectively not possible to avoid a coalescence between the flapping and bending modes. However the coalescence can be shifted to a higher airspeed by adjusting the wing tip hinge flare angle, which results in extra aerodynamic damping that can stabilise the flutter mechanism [4].

The test campaign was performed in the Airbus 12ft by 10ft low speed wind tunnel in Filton, UK. The interface between the inner wing and the detachable mid / outer wing provided an ideal anchor point to the wall of the wind tunnel, such that only the mid and outer part of the left wing was tested, plus both the 45m and 52m wing tips – figure 10 shows the wing installed in the wind tunnel. The anchor point allowed the wing angle of attack to be adjusted. A length of string was tied to a bracket on the underside of the wing tip, passed through the wing and the tunnel wall, and then pulled and released in order to provide the dynamic excitation for the first part of the test. An accelerometer was installed in the wing tip in order to measure the acceleration time history. For the second part of the test the wing tip coasting angle was recorded with a camera.



Figure 10: Wind tunnel test

The results from the first part of the test are shown in figures 11 and 12. Figure 11 provides an example result from the case with an airspeed of 18m/s and aircraft angle of attack of 4 degs. In both the acceleration time history and Fourier transform it can be seen that the response is dominated by the wing tip flapping frequency at approximately 3.5Hz. The wing bending frequency is at over 30Hz indicating a large frequency separation. Figure 12 gives the frequency of the flapping mode for both the 45m and 52m wing tips for the full range of airspeeds. The maximum frequency is less than 6Hz. However it should be noted that the first wing bending mode frequency of the full wing connected to the fuselage is approximately 15Hz rather than the 30Hz measured for the shortened wing in the wind tunnel. Nevertheless the frequency separation is still more than 9Hz indicating that the wing tip flapping mode cannot couple with the first wing bending to cause flutter. Figure 12 also shows that the wing tip flapping frequencies for the 52m wing tip are lower than for the 45m wing tip, which is as expected and due to the greater inertia of the 52m tip. Also as expected is the clear increase of the flapping frequency with airspeed.

The trend is not as linear as previous modelling for the full size aircraft has predicted [4] (note the apparent “dog leg” at 18m/s), but this is likely to be due to scatter in the results since the acceleration time histories were minimally processed in order to confirm there is no flutter risk.

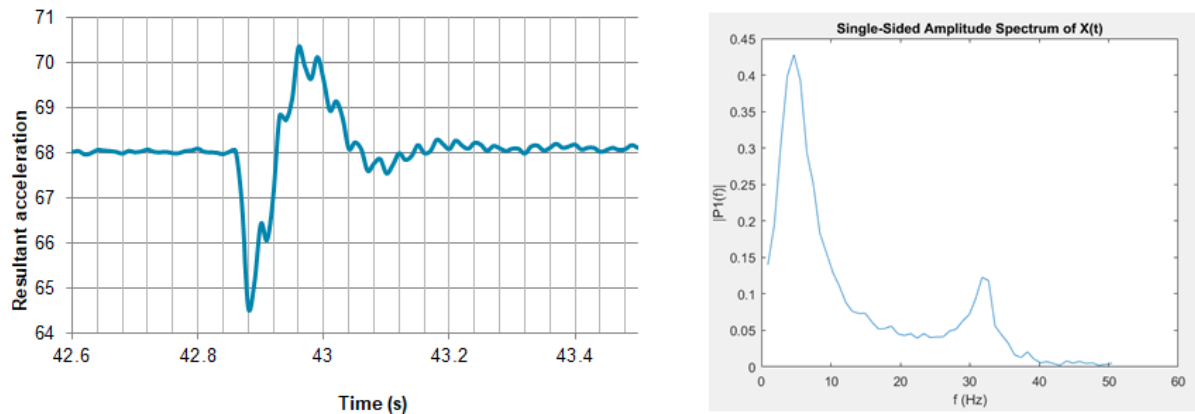


Figure 11: 45m wing tip release acceleration time history (left) and Fourier transform (right) at airspeed of 18m/s and aircraft angle of attack of 4 degs

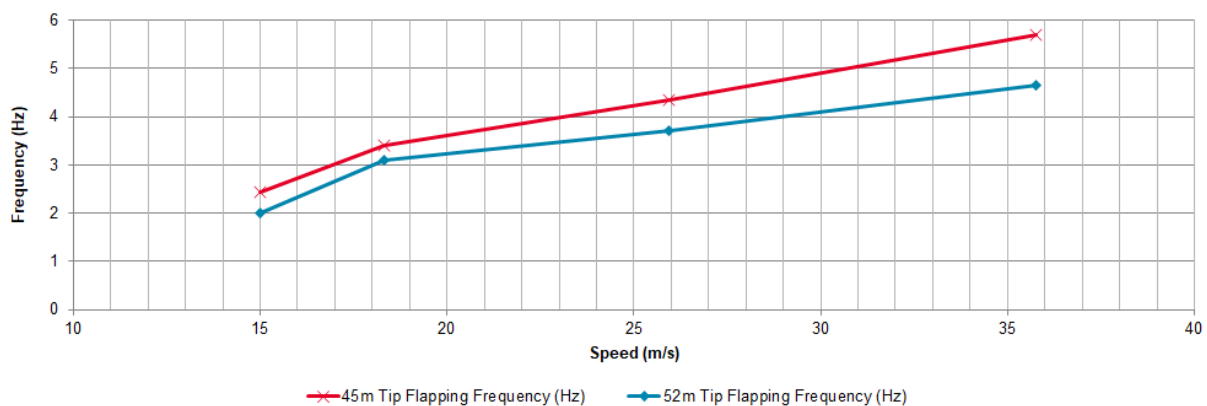


Figure 12: Flapping frequency for 45m and 52m wing tips versus airspeed

The results for the second part of the test are shown in figures 13 and 14, where the relationship between wing tip coasting angle and airspeed and aircraft angle of attack is shown. Figure 13 shows the coasting angles are less for the heavier 52m wing tip, and also that as the airspeed increases the coasting angle is asymptotic as the weight of the wing tips apparently becomes less significant. Figure 14 shows the expected increase in coasting angle with aircraft angle of attack. For low coasting angles the gradient of delta coasting angle to delta angle of attack is approximately 3 to 1, regardless of the size of the wing tip or the airspeed. At higher angles of attack the wing tip coasting angle appears to reach a maximum of no more than 45 degs. It is important to note that this non-linear behaviour is not the wing tip stalling – because of the zero moment across the hinge the wing tip only needs to generate enough lift to balance its weight (approximately 100 grams) in terms of hinge moment. Instead as the coasting angle increases the relationship between coasting angle and angle of attack (as a consequence of the flare angle) becomes weaker, and the effective side slip due to the flare angle (approximately 15 degs) becomes dominant. Of course this begs the question as to whether an aircraft in side slip could

result in the “effective” flare angle changing and affecting the behaviour of the free wing tips, and in the extreme if the side slip was greater than the flare angle whether the wing tips could become statically unstable. For this reason for the free hinge flight test cable ties were used to stop the wing tip coasting angle exceeding 90 degs.

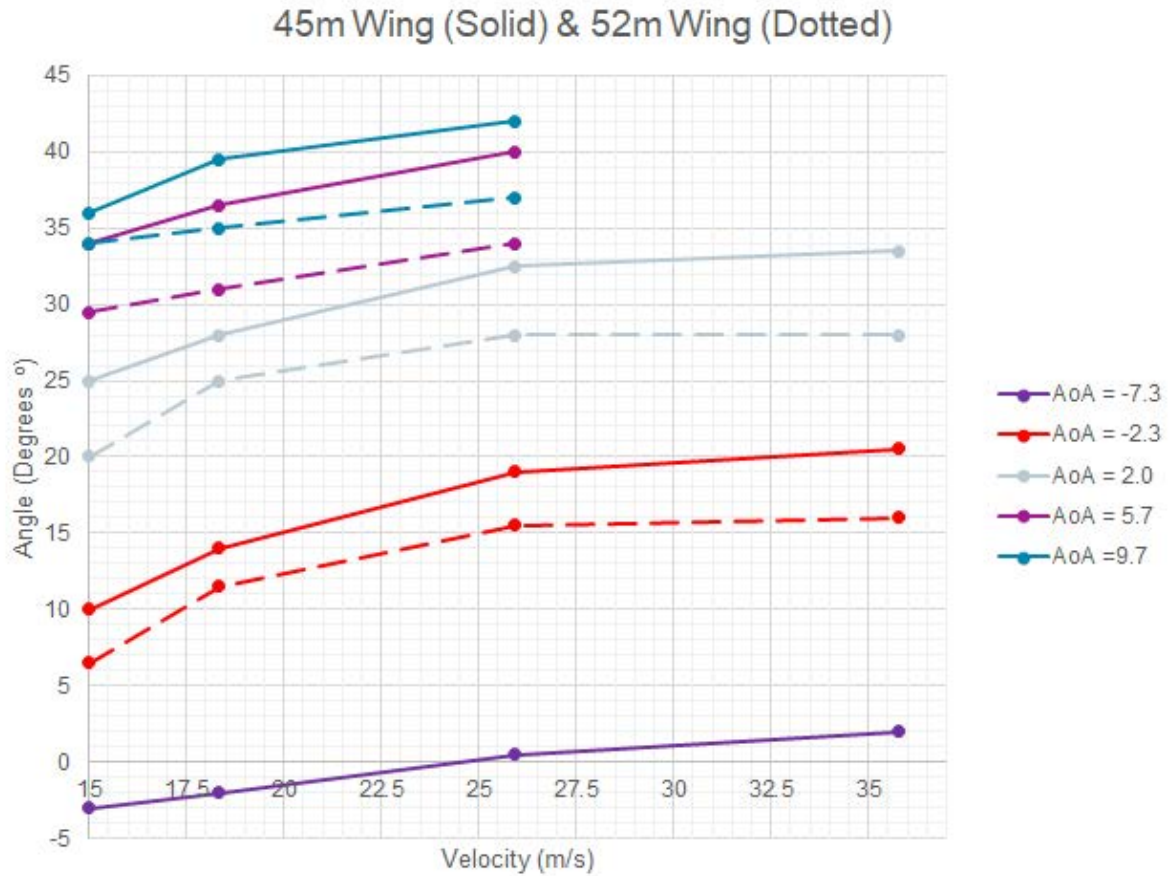


Figure 13: Coasting angle versus airspeed for 45m and 52m wing tips for a range in aircraft angle of attack

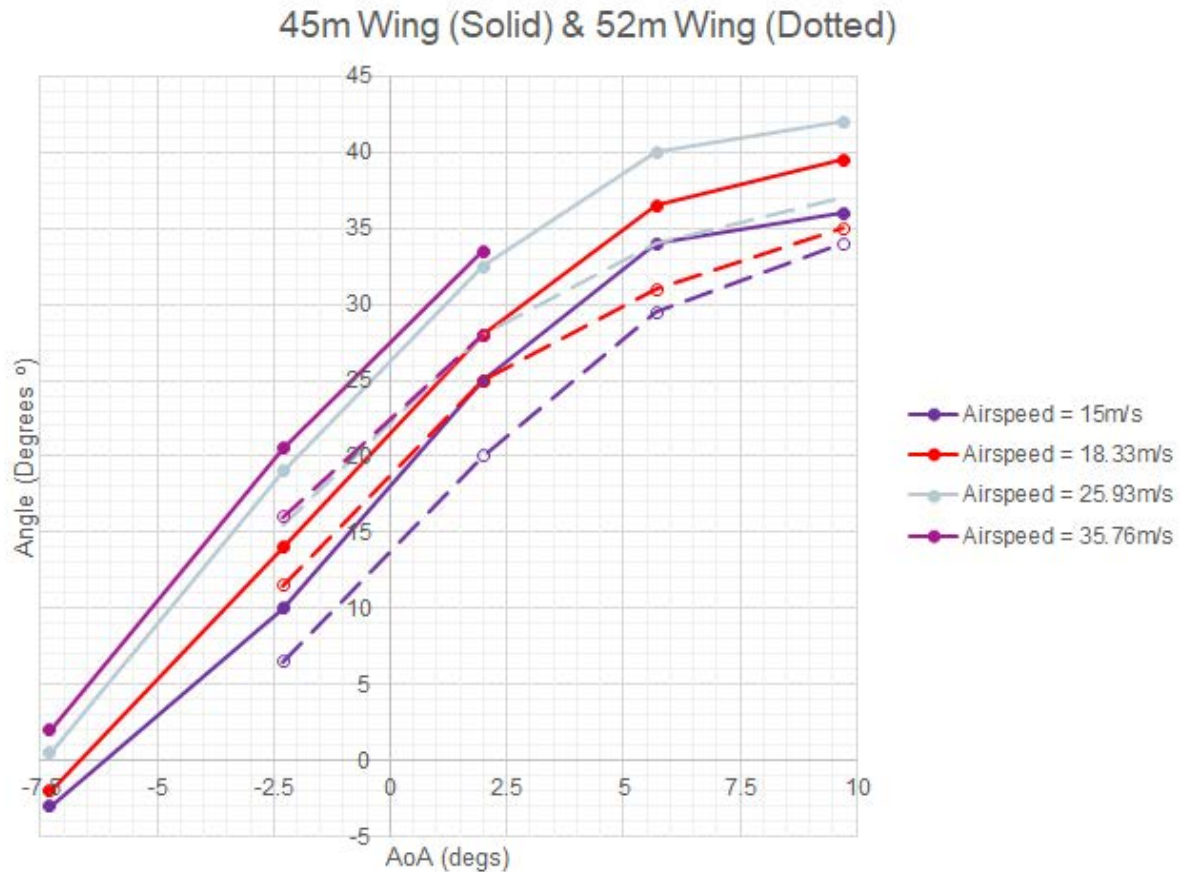


Figure 14: Coasting angle versus aircraft angle of attack for 45m and 52m wing tips for a range in airspeed

In addition to the measured data, a number of qualitative observations were made during the wind tunnel testing:

- Due to the very low turbulence in the wind tunnel the coasting behaviour of the free wing tip is almost complete steady for moderate aircraft angles of attack.
- If the angle of attack is increased so that the wing goes into stall, the wing tip remains unstalled and the motion required to maintain zero moment across the hinge is small.
- The force required to pull the wing tip back to its planar position with the string can be high (for the person pulling), especially for high angles of attack and/or high airspeeds.
- If the wind tunnel is started with the wing tip at a fold angle of approximately 135 degs the wing tip will “unfurl” once the airspeed becomes sufficiently high.

8. FLIGHT TESTS

Prior to the flight tests a number of ground tests were completed. These included wind tunnel testing, transmitter / receiver and telemetry tests, engine tests, FTI tests, and limit load static testing of the wings, wing tips, fuselage, HTP and VTP.

8.1 Flight test philosophy

The philosophy for the flight tests is diagrammatically shown in figure 15. The philosophy was developed to step through the flight test campaign so that the low risk elements came first and

the most risky last. Practically this meant ground run tests before flying, including handling, rejected take-offs and rotations; Flying with fixed wing tips before free wing tips; Flying free wing tips before attempting to release and then recover the wing tips in flight; And flying with the 45m wing tips before the 52m wing tips.

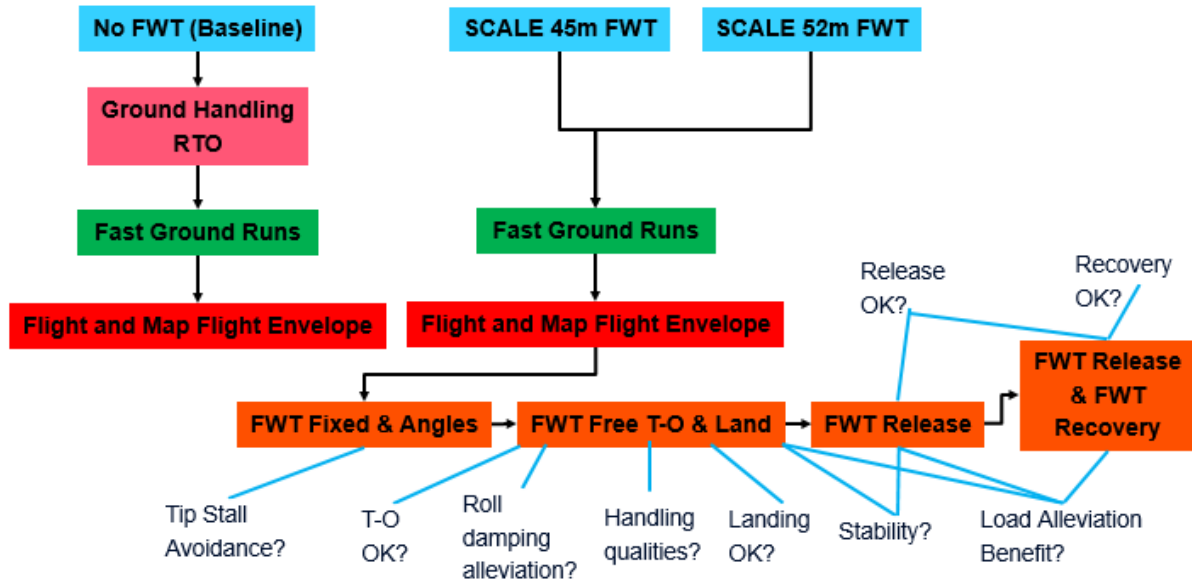


Figure 15: Flight test philosophy

After all the ground run tests had been completed, the above philosophy was adapted for the first phase of flight testing: It was decided to fly twice with the 45m wing tips, fixed and then free.

8.2 Summary of the flight tests

The first two flights were performed on 26th February 2019 at Aston Down airfield in Gloucestershire, UK. For each flight the aircraft performed a series of left hand circuits, in “clean” and “high lift” configurations, and including stall tests. The flight time for both flights was approximately five minutes, and the aircraft stayed below 25m/s and within the operational area in terms of 500m from the pilot and no more than 400ft altitude. Figure 16 shows images from the flight tests.



Figure 16: Images from the flight tests

8.3 Results

The first findings from the flight tests were qualitative:

- The wing tips were statically and dynamically stable throughout the flight.
- The wing tips “coasted” with no oscillations in calm air, but responded to gusts to maintain the zero hinge moment condition.
- The wing tip coasting angle tended to be higher in the turns when the angle of attack increased.

- The free wing tips gave the pilots no particular problems with controlling the aircraft.

The strain gauge results at spanwise stations of 35% and 56% are summarised in figure 17. The plots show the expected positive correlation between bending moment and aircraft load factor, although there is significant scatter. The scatter is due to the fact that the aircraft is very light and so gets “buffeted” by small gusts, plus the general the level of unsteadiness was quite high – for example no attempt was made to achieve totally stable level flight or precisely coordinated turns, although landing, take-off and stall tests were filtered from the data. Despite the scatter it is clear that the bending moments at these two spanwise stations are lower for flight 2 than for flight 1, thus confirming the load alleviation effect.

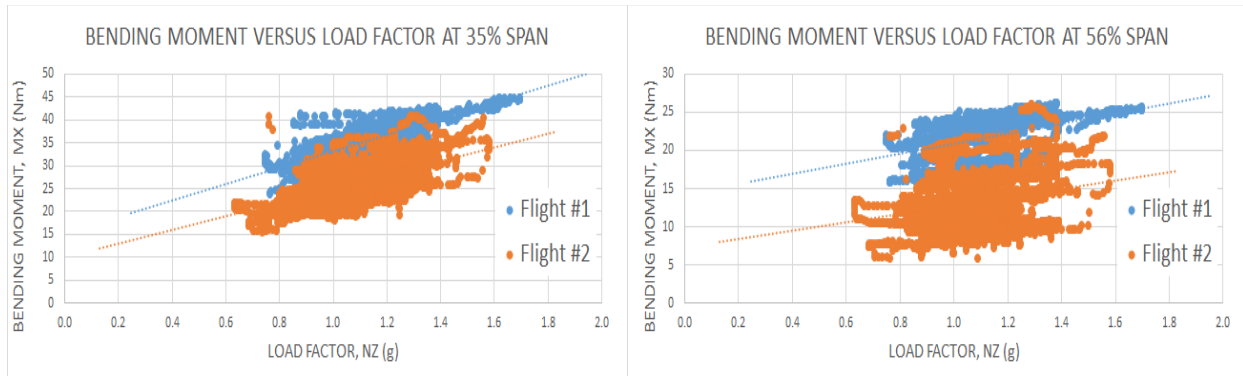


Figure 17: Bending moment versus aircraft load factor at 35% and 56% span for flight #1 (fixed wing tip) and flight #2 (free wing tip)

Due to problems with the wing tip accelerometers, which could also be used as inclinometers, another means was required to record the coasting angles for the free wing tips. This was achieved by writing software to process the VTP video footage. Figures 18 to 20 show the results. Figure 18 shows the relationship between wing tip coasting angle (average of left and right) and aircraft angle of attack, and despite the scatter the data confirms the wind tunnel results including the geometric non-linear behaviour. Additionally a simple geometric calculation of the change in coasting angle due to the change in aircraft angle of attack, as defined in equation (1), shows excellent agreement with the wind tunnel results in the linear region. The time histories of the left and right wing tips is shown in figure 19. There is a clear asymmetry between the two wing tips, which is currently not understood, but is possibly due to interference from the cable ties that were installed at the hinge to prevent the wing tip coasting angle exceeding 90 degs. Figure 20 is a zoom of the wing tip time histories and displays the response to a gust.

$$\Delta\theta = \tan^{-1}(\tan\Delta\alpha / \sin\Lambda) \quad (1)$$

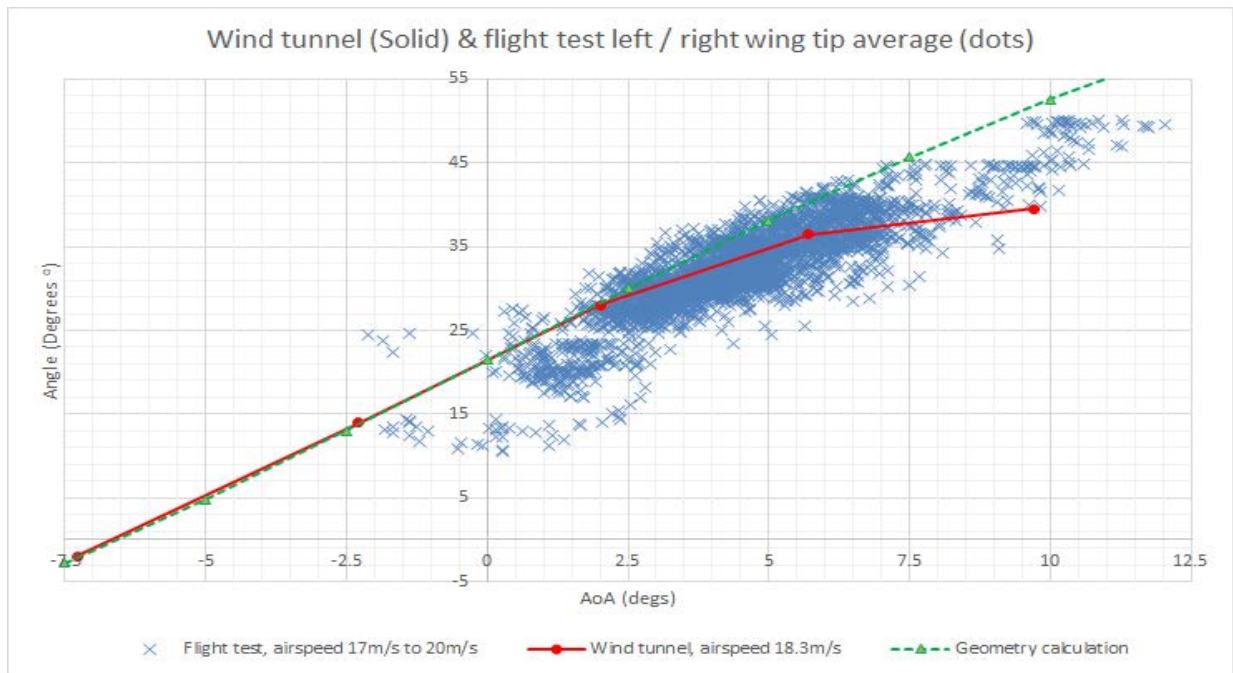


Figure 18: Average of left and right wing tip coasting angles versus aircraft angle of attack for flight #2, plus wind tunnel result, plus geometry calculation

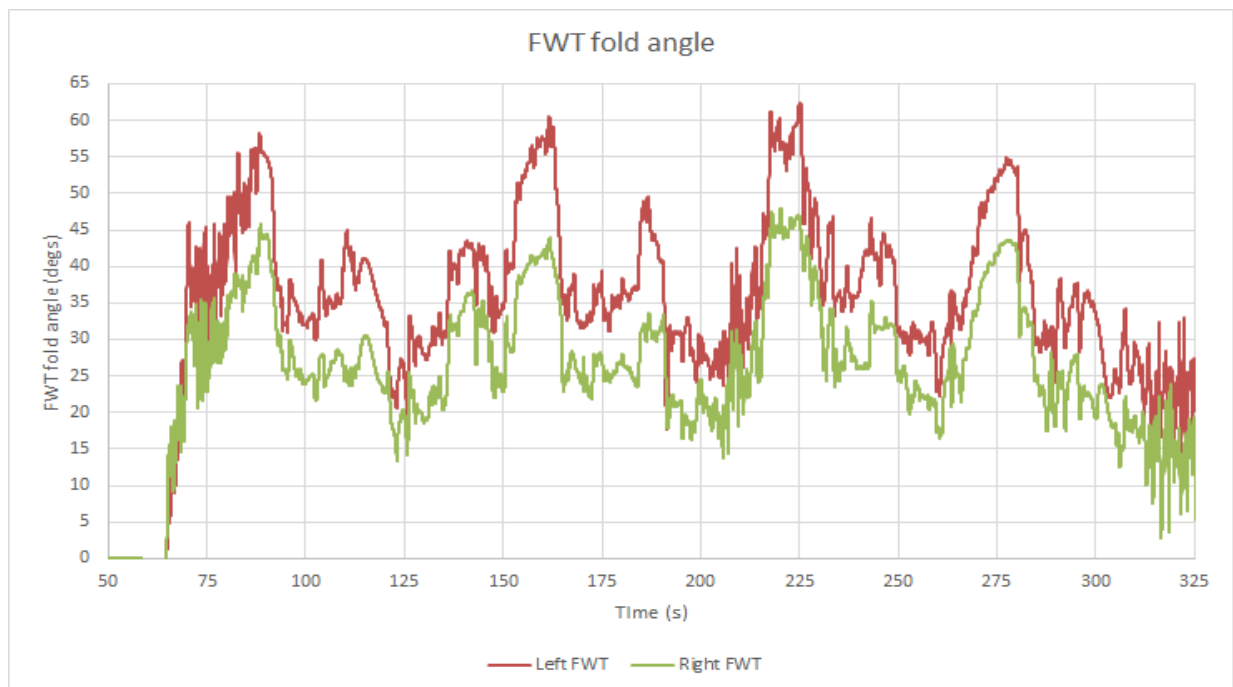


Figure 19: Left and right wing tip coasting angles versus time for flight #2

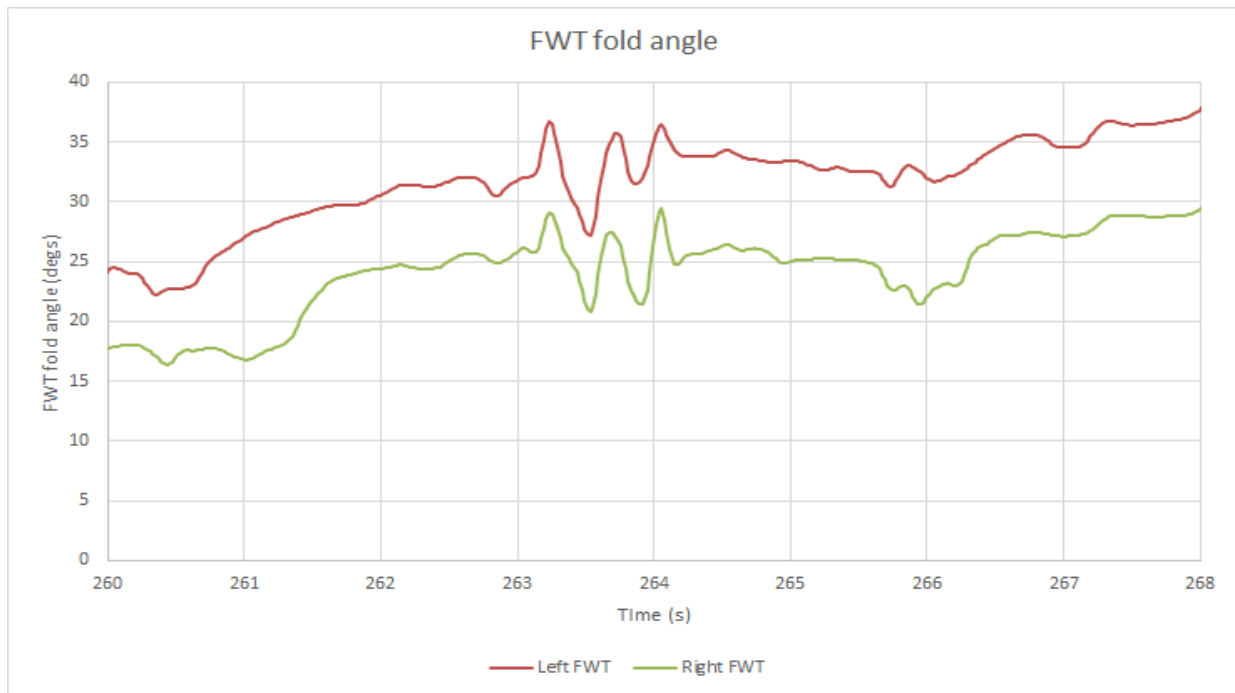


Figure 20: Left and right wing tip coasting angles versus time for flight #2 – zoom showing response to a gust

9. CONCLUSIONS

The second flight of AlbatrossONE represented the first ever flight of an aircraft with free folding wing tips, and throughout the flight the wing tips were demonstrated to be both statically and dynamically stable. The wing load alleviation effect from the free wing tips has been confirmed through comparing the strain gauge measurements between the two flights. The coasting (free folding) angle of the wing tips has been shown to have a non-linear relationship with aircraft angle of attack because the hinge flare angle causes an effective sideslip. And the near linear variation of wing tip flapping frequency with airspeed was confirmed by the wind tunnel tests. In general the first flights of AlbatrossONE represent a major step in demonstrating that the Semi Aeroelastic Hinge technology is a serious proposition.

10. NEXT STEPS

The flight test campaign will be completed with the following elements:

- Identify the roll damping alleviation effect due to freely hinged wing tips.
- Identify the tip stall avoidance effect due to freely hinged wing tips (in flight).
- Fly with the 52m wing tips fixed & free.
- Fly with no wing tips.
- Release the wing tips in flight.
- Recover the wing tips to their planar position in flight.

In addition the mathematical models of AlbatrossONE require significant improvement. The models (e.g. finite element model, loads model, longitudinal trim and handling qualities model) that have been developed to date are relatively simple and were created to give the data needed to produce a conservative design. They are however not adequate for properly understanding the physical behaviour of the aircraft, and the wing tips in particular (noting the non-linear geometric

effect as the coasting angle increases). There is much still to learn about the physical behaviour of free hinged / semi aeroelastic wing tips, and better models allied to the AlbatrossONE flight test data will enable this.

11. ACKNOWLEDGEMENTS

Many thanks to all the colleagues who have worked on or supported this topic recently, including Andy Dyer, Alex Fordham, Manuel Taramona Perez, Thomas Maierhofer, Rob Buckley, Raymond (Hao Chen) Yu, Alvaro Azabal, Kirsty Mon Williams, John Yorke, Colin Atwell, Mike Bishop, Hagen Christian Hagens, Jan-Niklas Garbers, Sylwia Kozłowska, Ed Wheatcroft, Carmine Valente, Patrick Metcalfe, Reece King, Paul Kealy, Anna Delmas, Jessica Kiraly, Joshua Robson, Abdul Rehman, Kushal Agarwal, Andy McCarthy, Med Evans, Ciaran O'Rourke and Simon Galpin all at Airbus, plus Jonathan Cooper at the University of Bristol, and Mudassir Lone and Gaetan Dussart at Cranfield University.

12. REFERENCES

- [1] Aeroelastic Behaviour of Hinged Wing Tips; T. Wilson, M. Herring & A. Azabal, Airbus; A. Castrichini & J. Cooper, University of Bristol; and R. Ajaj, University of Southampton; IFASD 2017
- [2] An aircraft wing with a moveable wing tip device for load alleviation, patent application GB2546246A; T. Wilson, M. Herring, J. Pattinson, J. Cooper, A. Castrichini, R. Ajaj, H. Dhoru, July 2017
- [3] Preliminary Investigation of Use of Flexible Folding Wing-Tips for Static and Dynamic Loads Alleviation; A. Castrichini, V. Siddaramaiah, D. Calderon, J. Cooper, T. Wilson, Y. Lemmens, *Aeronautical Journal - New Series*, published online 21 Nov. 2016, Doi: 10.1017/aer.2016.108
- [4] Aeroelastic Behaviour of Hinged Wing Tips; T. Wilson, M. Herring & A. Azabal, Airbus; A. Castrichini & J. Cooper, University of Bristol; and R. Ajaj, University of Southampton; RAeS 5th Aerospace Structures Design Conference, 2016
- [5] Nonlinear Folding Wing-Tips for Gust Loads Alleviation; Castrichini, A., Hodigere Siddaramaiah, V., Calderon, D., Cooper, J., Wilson, T. & Lemmens, Y.; *Journal of Aircraft*, published online 17 Feb 2016. Doi: <http://dx.doi.org/10.2514/1.C033474>
- [6] High fidelity simulation of the folding wing tip, J. Pattinson, M. Herring & T. Wilson Airbus Group Innovations/ Airbus, IFASD 2015
- [7] Nonlinear Negative Stiffness Wing-Tip Spring Device for Gust Loads Alleviation; Castrichini, A., Cooper, J. E., Wilson, T., Carrella, A. & Lemmens, Y; *Journal of Aircraft*, published online 9 Nov. 2016. Doi: 10.2514/1.C033887
- [8] Wind Tunnel Testing of Folding Wing-Tip Devices for Gust Loads Alleviation; R. Cheung, A. Castrichini, D. Rezgui & J.E. Cooper, University of Bristol; and T. Wilson, Airbus; IFASD 2017
- [9] Anatomy and histochemistry of spread-wing posture in birds. 3. Immunohistochemistry of flight muscles and the “shoulder lock” in albatrosses; Ron A. Meyers & Eric F. Stakebake, *Journal of Morphology* 2004
- [10] The Dynamic Release of the Semi Aeroelastic Hinge Wing-Tip Device; A. Castrichini & T. Wilson; And J., University of Bristol; RAeS 6th Aerospace Structures Design Conference, 2018
- [11] Non-Linear Aeroelastic Behaviour of Hinged Wing Tips; T. Wilson & A. Castrichini, Airbus; J. Paterson & R. Arribas, formerly Imperial College London; RAeS 6th Aerospace Structures Design Conference, 2018

COPYRIGHT STATEMENT

The authors confirm that they, and/or their company or organisation, hold copyright on all of the original material included in this paper. The authors also confirm that they have obtained permission, from the copyright holder of any third party material included in this paper, to publish it as part of their paper. The authors confirm that they give permission, or have obtained permission from the copyright holder of this paper, for the publication and distribution of this paper as part of the IFASD-2019 proceedings or as individual off-prints from the proceedings.